

Microscopic structure factor of liquid hydrogen by neutron-diffraction measurementsM. Celli,¹ U. Bafle,¹ G. J. Cuello,² F. Formisano,³ E. Guarini,⁴ R. Magli,^{5,6} M. Neumann,⁷ and M. Zoppi¹¹*Consiglio Nazionale delle Ricerche-Istituto dei Sistemi Complessi, Via Madonna del Piano, I-50019 Sesto Fiorentino, Italy*²*Institut Laue-Langevin, 6 rue J. Horowitz, BP 156, F-38042, Grenoble Cedex 9, France*³*Istituto Nazionale per la Fisica della Materia-Operative Group in Grenoble, c/o Institut Laue-Langevin, 6 rue J. Horowitz, F-38042, Grenoble Cedex 9, France*⁴*Istituto Nazionale per la Fisica della Materia-Unità di Firenze, Via G. Sansone 1, I-50019 Sesto Fiorentino, Italy*⁵*Dipartimento di Chimica, Biochimica, e Biotecnologie per la Medicina, Università di Milano, Via F.lli Cervi 93, I-20090 Segrate, Italy*⁶*Istituto Nazionale per la Fisica della Materia-Unità di Milano, Via Celoria 16, I-20133 Milano, Italy*⁷*Institut für Experimentalphysik, Universität Wien, Strudlhofgasse 4, A-1090 Wien, Austria*

(Received 1 October 2004; published 19 January 2005)

The center-of-mass structure factor of liquid para hydrogen has been measured, using neutron diffraction, in four thermodynamic states close to the triple point. Path integral Monte Carlo simulations have been carried out at the same temperatures and densities. The present experimental data are in reasonable quantitative agreement with the simulations and closer to these results than previous neutron determinations available in the literature. The thermodynamic derivatives of the structure factor, from both experiment and simulation, have been compared to previous measurements obtaining a quantitative consistency.

DOI: 10.1103/PhysRevB.71.014205

PACS number(s): 61.12.-q, 67.20.+k, 61.20.Ja

I. INTRODUCTION

Hydrogen isotopes, neon, ⁴He above the superfluid transition, and ³He above the Fermi temperature are representative of the class of quantum Boltzmann liquids, while superfluid ⁴He is a good example of a Bose liquid and cold ³He is the prototype of a Fermi liquid. Boltzmann liquids are characterized by rather large quantum effects, which show up in the noncommutative character of the center of mass momentum and position operators, even though the individuality of the single particles (either atomic, for the case of helium and neon, or molecular, for the case of the hydrogens) is retained. While the weak quantum properties of neon can be reproduced rather accurately using an asymptotic expansion (e.g., Wigner-Kirkwood), starting from a classical reference system,¹ a similar perturbative approach does not hold for the hydrogen isotopes, nor for liquid ⁴He above the λ transition.² In addition, the low critical temperature of ⁴He ($T_c=5.2$ K) makes its liquid interval rather narrow. Thus, the hydrogen isotopes represent the most relevant example of a Boltzmann quantum liquid and an experimental benchmark for the Boltzmann liquid theories. It is worthwhile to mention that the microscopic dynamics of such a quantum liquid is still an open problem in physics^{3,4} and that the structural information is a fundamental ingredient of any dynamic theory.⁵

A precise knowledge of the structural and dynamic properties of hydrogen is even more desirable if one considers its growing importance as a proposed energy carrier for a not too far future of our planet. As a matter of fact, even though the liquid phase of hydrogen is not the best candidate to store energy, from a purely energetic-balance point of view, nevertheless, it can be foreseen that it will likely constitute an important intermediate stage in the next hydrogen-economy society. However, in spite of its apparent simplicity, the structure factor $S(k)$ of liquid hydrogen is not yet known

with the precision that would be desirable, for example, to build a reliable dynamic theory. This is a consequence of several experimental problems.

Two microscopic tools give access to the structural properties of liquids: x rays, which are sensitive to the electron clouds of the atomic or molecular samples, and thermal neutrons, which can probe directly the positions and motions of the nuclei. Due to the recent advance of synchrotron radiation sources, even small cross-sectional samples can be investigated with some success. However, as the hydrogen molecule carries only two electrons, the structural determination using x rays does not appear an easy task, also because of the presence of the molecular form factor, which depresses the scattering cross section in the high-momentum transfer region. Neutron-diffraction experiments are difficult, too, because of the presence of large contributions from both inelastic and incoherent scattering, for which the experiment data should be corrected. As far as inelastic effects are concerned, apart from the presence of the intramolecular energy levels that might be excited at the expense of the incident neutron energy, their importance is determined by the ratio between the neutron and the nuclear mass, which makes the standard correction techniques⁶ inadequate in the hydrogen case. Due to its double nuclear mass, deuterium appears to be more suitable for a neutron investigation. In fact, diffraction experiments on D₂ have been shown to be feasible, even though the first reliable data are relatively recent.⁷⁻¹⁰

The overwhelming ratio between the incoherent and coherent neutron-scattering cross section of the protons is the other main problem in a neutron-diffraction study of the structure of liquid hydrogen, since the intermolecular response, which carries the structural information, is overpowered by a large intramolecular contribution coming from the single-molecule structure and dynamics. Thus, even the smallest instrumental instability would contribute to mask the sought-for intermolecular structure. In fact, a successful attempt to obtain structural information on liquid hydrogen

was carried out measuring differential quantities, such as the thermodynamic derivatives of $S(k)$.¹¹ The smaller amount of incoherent scattering makes neutron diffraction easier on deuterium. However, the knowledge of the deuterium structure factor is not readily transferred to hydrogen because of the different role played by quantum effects.¹²

At the typical temperatures of the liquid phase, if thermal equilibrium is achieved, then practically all hydrogen molecules belong to the paraspecies. Since the molecular neutron-scattering cross sections are different for the para- and orthospecies, it is important to be sure that the equilibrium composition is reached before starting the measurement. As the spontaneous conversion from ortho- to parahydrogen is rather slow¹³ and depends on the shape and composition of the container, it is always convenient to speed up the conversion rate by adding a suitable catalyst. In this way, one makes sure that the sample composition is stable in time and, in addition, the calculation of the intramolecular features are simplified (practically, only the lowest rotational state, $J=0$, is populated). Therefore, all neutron experimental work is actually done on parahydrogen.

Various methods have been suggested to overcome the experimental problems that hinder a structure determination in liquid parahydrogen. On the one side, pulsed neutron time-of-flight (TOF) diffraction could be used. By this technique, keeping the scattering angle small enough, it is possible, at least in principle, to make the inelastic effects so small that they can be dealt with as small corrections.⁷ However, this technique is limited by the present overall stability of the available instrumentation operating at a pulsed-neutron source.¹¹ Another possibility is to rely on the intrinsically more stable instrumentation of a reactor neutron source. However, in this case, the need of reaching a large scattering angle to cover a sufficiently extended k range implies the emergence of large inelastic effects that influence the measured cross section.

Alternatively, Bermejo *et al.*¹⁴ resolved to determine the structure factor of liquid hydrogen using the results of a neutron-inelastic-scattering experiment and the sum rule that relates the static and dynamic structure factors¹⁵

$$S(k) = \int_{-\infty}^{+\infty} d\omega S(k, \omega). \quad (1)$$

The results, though qualitatively reasonable, do not appear to be fully convincing.¹⁶ In fact, the measured structure factor is at variance with path integral Monte Carlo¹⁷ (PIMC) simulations and the main peak of $S(k)$ turns out rather high, close to the value of 2.85, which marks (according to the Hansen-Verlet criterion,¹⁸) the onset of the freezing transition for a classical Lennard-Jones liquid.¹⁶

A different route was recently exploited by Dawidowski *et al.*¹⁹ who used low-energy neutrons from a reactor source to perform a diffraction experiment. By this technique, the incident neutron energy is so small that it cannot excite the first rotational transition of molecular hydrogen. Thus, the incoherent scattering power of the sample is greatly reduced.^{15,19} However, even this technique bears its prob-

lems. For example, using small energy neutrons, the available k range does not allow one to use an internal calibration procedure ($S(k)=1$ in the high- k limit) and this imposes the need of relying on an external intensity calibration (typically, a vanadium sample). In addition, the limited size of the incident neutron momentum $\hbar k_0$ produces a ratio k_1/k_0 (i.e., between the scattered and incident wave vector, respectively) farther from unity than in a standard diffraction experiment. This makes the static approximation totally useless for these experimental conditions and implies a substantial correction to the measured data. It is worthwhile to observe that, in order to calculate this correction, a model for the inelastic scattering law is needed.¹⁹ The authors of Ref. 19 have properly accounted for all these problems. However, the reported results appear, to some extent, influenced by the theoretical model used in the analysis procedure.

For the sake of completeness, it is interesting to mention that the method of integrating the dynamic structure factor at constant k was recently applied by Pratesi *et al.* to x-ray scattering data obtained in a synchrotron-radiation inelastic experiment.²⁰ The reported data are not much extended in k , barely exceeding the main peak position of $S(k)$ and with rather large error bars. However, different from Ref. 14, the main peak is found to be consistent with the quantum-mechanical PIMC simulations carried out by the same authors.²⁰ The same experimental team reported the results of an x-ray-diffraction measurement, too, with much smaller error bars and still a good agreement with their quantum-mechanical simulations.²⁰

As each experimental method has advantages and disadvantages, it is highly desirable that the information originating from the various experimental techniques be critically compared in order to increase, as much as possible, the degree of confidence in the results. With this in mind, we report the results of a neutron-diffraction experiment on liquid parahydrogen ($p\text{-}^1\text{H}_2$), in various thermodynamic conditions, carried out on a standard liquids diffractometer at a reactor source. The present results will be compared to the available experimental data, as well as with our own PIMC simulations, carried out at the same densities and temperatures. In Sec. II, we will discuss the details of the present experiment, while Sec. III will be devoted to describe the data analysis. In Sec. IV the PIMC simulation technique will be outlined and, in Sec. V, we will compare and discuss the various results. The conclusions will be drawn in Sec. VI.

II. EXPERIMENT

The measurements were performed using the D4C diffractometer at the Institut Laue-Langevin (ILL, Grenoble, France) with an incident wavelength $\lambda_0=0.6933 \text{ \AA}$. Four thermodynamic states of liquid parahydrogen were investigated and will be referred to, in the following, by the labels given in the first column of Table I. After performing the usual runs (i.e., vanadium calibration, empty cryostat, and empty cell), hydrogen was condensed into a vanadium cylindrical container (6 mm internal diameter, 0.2 mm wall thickness) cooled in an Orange ILL cryostat. At the bottom of the container, out of the neutron beam, we had inserted some

TABLE I. Thermodynamic conditions of the measured parahydrogen liquid samples. The densities have been derived using the equation of state in Ref. 21. The values of $S(0)$ are obtained from the thermodynamic compressibilities.

No.	T (K)	p (bar)	n (nm ⁻³)	$S(0)$
1	17.1(1)	29.9(1)	22.95(3)	0.059(1)
2	17.1(1)	16.2(1)	22.60(3)	0.065(1)
3	20.1(1)	16.4(1)	21.78(4)	0.094(1)
4	18.6(1)	16.2(1)	22.20(3)	0.079(1)

powder of a paramagnetic catalyst (Cr_2O_3 on an Al_2O_3 substrate) in order to speed up the conversion from ortho- to parahydrogen. The concentration of the two species was monitored by looking at the low-momentum transfer portion of the diffraction pattern.¹¹ After 24 h of conversion time, the stability of the low- k signal confirmed that the sample had reached the thermal equilibrium concentration, calculated to be 99.96% rich in parahydrogen. For each thermodynamic state, several measurements, in repeated runs, were carried out to check the overall stability of the experimental setup, as well as of the sample. The overall temperature stability was much better than 0.1 K. However, according to the sensor characteristics, we assumed an error of 0.1 K in the temperature reading. A similar protocol was adopted for the pressure reading, assuming an absolute error of 0.1 bar with a pressure stability much better than this amount. Densities were determined by the equation of state of Ref. 21.

In order to properly subtract the background and container scattering, we made an additional measurement, without changing the experimental setup, filling the container with a small amount of gaseous ^3He . The density of the gas was chosen such as to match the attenuation of parahydrogen with the absorption power of ^3He . The details of the procedure can be found in Ref. 22. We used the value $\sigma(\lambda_0) = 43.4$ barn for the molecular hydrogen-scattering cross section at the incident-neutron wavelength.²³ In Fig. 1, we show the measured intensity for state 1 ($T=17.1$ K and p

$=29.9$ bar), after subtraction of the instrument background and container scattering properly corrected for attenuation. We point out that the size of the statistical error is smaller than the symbols.

The shape of the measured cross section does not look familiar for a molecular liquid. However, this is what one would expect, qualitatively, for liquid parahydrogen on a reactor neutron source. In fact, the diffraction spectrum is dominated by the *self* molecular part, which is produced by the intramolecular structure (cf. Fig. 1 of Ref. 11). In addition, the finite energy of the incident neutron imposes kinematic restrictions, which, in turn, produce the decay observed at high-momentum transfer. The *distinct* contribution, containing the required information on the intermolecular structure factor, appears as a tiny undulation superimposed on the much larger intramolecular structure in the region $k \approx 2 \text{ \AA}^{-1}$.

III. DATA ANALYSIS

The intermolecular structure can be expressed in terms of either the center-of-mass or the site-site structure factor. These two quantities are directly related to each other²⁴ in the free-rotation approximation that will be used below for hydrogen. We chose to express our results in terms of the center of mass $S(k)$ for consistency with previous results and for ease of comparison with the PIMC simulation, where the center-of-mass structure is the natural output. The data treatment needed to extract the structure factor requires the calculation of the *self* part of the molecular double-differential neutron cross section of parahydrogen. This can be done using the Young and Koppel (YK) theory.²⁵ Here, the hydrogen molecules are modeled as a set of noninteracting particles possessing their relevant internal degrees of freedom. Thus, each molecule is considered separately, and the intramolecular roto-vibrational modes and spin correlations are explicitly taken into account. The vibrational modes are considered harmonic, and the rotations are free. This model applies to our case because, as long as the system is in the fluid phase,

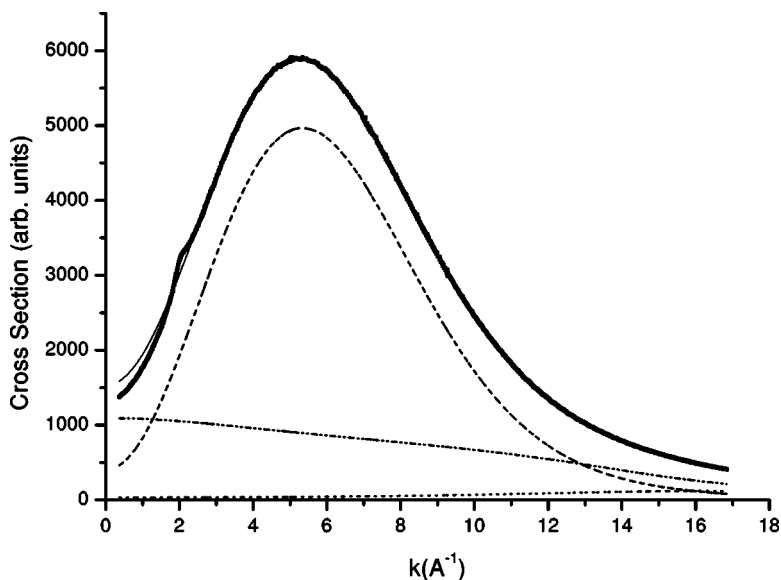


FIG. 1. Diffraction intensity from liquid parahydrogen at $T=17.1$ K and $p=29.9$ bar. What in the figure appears as a bold line is composed, instead, by the ensemble of the experimental points and their error bars (of the order of 0.1 %). The tiny structure in the region $k \approx 2 \text{ \AA}^{-1}$ is the signature of the main peak of the intermolecular structure factor $S(k)$. The dashed line is the calculated self-molecular part, the dash-dotted line represents the Monte Carlo calculation of multiple scattering, and the dotted line is the fitted background. The thin solid line is the sum of the three terms.

the anisotropic components of the intermolecular potential have negligible effects.^{26–28} Moreover, at low temperatures, only the ground vibrational and rotational states are populated and, using thermal neutrons, no vibrational transition is allowed. Within the applicability limits of this model, a rigorous calculation of the double-differential neutron cross section is possible. However, since the YK model neglects intermolecular interactions, it is known to be inadequate to describe the center-of-mass dynamic structure factor $S_{self}(k, \omega)$ in dense hydrogen.

We have shown²³ that a modified Young and Koppel (MYK) model can be defined that allows, in a mean-field-framework approximation, to extend its applicability range to the dense fluid phase of interacting molecules. It is well known that for hydrogen, due to quantum effects, the average center-of-mass kinetic energy is different from the classical value $\langle E_k \rangle = \frac{3}{2}k_B T$ and depends on density.²⁹ To account for this property we used an effective temperature ($T_{eff} = 41$ K, as measured in a neutron-inelastic-scattering experiment)³⁰ in the width of the Gaussian that describes the dynamic structure factor of the molecular centers of mass.²³ The vibrational-rotational coupling too can be accounted for, in an effective way, using the experimental values for the rotovibrational energies.³¹ The *self* portion of the double-differential neutron cross section, calculated with the MYK model, can be integrated, for each scattering angle θ , over the energies of the scattered neutrons. The result, properly normalized as described below and corrected for attenuation, detector efficiency, and for finite-size effects of sample and detectors, is represented by the dashed line in Fig. 1.

A thorough analysis of the measured cross section, in the region of $k \approx 5 \text{ \AA}^{-1}$, shows a slight variance of the peak position with respect to the MYK calculation in all the measured spectra. This cannot be attributed to the calibration of the instrument k scale, as it was checked by the position of the tiny Bragg peaks of the empty container. Therefore, we are forced to attribute this slight variance to the not-perfect adequacy of the MYK model in accounting for the *self* term of the parahydrogen cross section in the liquid state.

With respect to the MYK calculation, we observe an extra intensity in the measured data. The similarity in shape between the measured pattern and the calculated intramolecular cross section indicates the presence of a rather unstructured background, which is expected to be mostly due to multiple scattering. In order to properly subtract this unwanted contribution, we performed a Monte Carlo simulation of the multiple scattering, using as input the calculated MYK cross section. As expected, we obtained a smooth function of k , also reported in Fig. 1 (dash-dotted line). At this point, the main ingredients were available and we could proceed to determine the intermolecular center-of-mass structure factor. A model function was built according to

$$I_{exp}(\theta) = A \left[\left(\frac{d\sigma}{d\Omega} \right)_{self}^{att,SE} + A_{s,sc}(k) \left(\frac{d\sigma}{d\Omega} \right)_{dist} + B(k) \right], \quad (2)$$

where A is an overall normalization parameter. The *self* term is the result from the MYK calculation, attenuated by the self-absorption (label *att*) and corrected for detector effi-

ciency and size effect of detectors and sample (label *SE*). The *dist* term represents the intermolecular structural response, which is multiplied by its relevant Paalman-Pings³² attenuation coefficient. For parahydrogen, the *distinct* cross section can be written as³³

$$\left(\frac{d\sigma}{d\Omega} \right)_{dist} = u(k)[S(k) - 1], \quad (3)$$

where $u(k)$ is the molecular form factor³³ and $S(k)$ is the unknown center-of-mass structure factor.

In Eq. (2), $B(k)$ represents a background term, which includes the calculated multiple-scattering contribution as well as a possible residual background modeled by an even polynomial in k , $P(k^2)$. Equation (2) was fitted to the corrected experimental data shown in Fig. 1, using A and the coefficients of $P(k^2)$ as free parameters. As the model function contains $S(k)$, which represents our final goal, we removed from the fit range an interval $k_{min} \leq k \leq k_{max}$ that is expected to be affected by the presence of the structure factor. Thus, we used only those data points where an independent knowledge of $S(k)$ is available. In the low- k region, we assumed a constant value for $S(k)$ determined by the isothermal compressibility. In other words, we approximated, in Eq. (3), $S(k) = S(0)$ for the data points belonging to the interval $0 \leq k \leq k_{min}$. For the data points at $k \geq k_{max}$, we approximated the structure factor by its high- k limit value (i.e., we assumed $S(k) = 1$).

A third-order polynomial $P(k^2)$ was found sufficient to describe the background (dotted line in Fig. 1) that, as expected, turned out quite smaller than the multiple-scattering intensity, confirming that the latter was calculated with good accuracy. The goodness and stability of the fit was also analyzed as a function of k_{max} , with k_{min} kept at 0.5 \AA^{-1} . A good stability could be obtained for k_{max} in the range $4-5 \text{ \AA}^{-1}$. The results from the PIMC simulation confirm that, in this region, $S(k)$ is already sufficiently close to 1 so that the coherent term could be safely neglected with respect to the average size of the experimental errors.

A final comment should be devoted to the calculation of the intramolecular contribution. As we have already mentioned, the MYK model does not give a quantitatively precise description of the *self* cross section of parahydrogen, even though its accuracy turns out to be rather good. In our case, we find that the maximum position of the calculated self-contribution does not coincide (by a mere $\approx 0.15 \text{ \AA}^{-1}$) with the experimental determination. In order to circumvent the problem and to produce a theoretical calculation closer to the experimental data, we decided to allow a slight variation of the equilibrium distance between the two protons in the MYK model. By this expedient, allowing for a slightly higher value for the intramolecular distance ($\approx 4\%$ higher than the free-molecule gas value in the ground state, $R_e = 0.741 \text{ \AA}$) we were able to obtain a small change in the position of the maximum, with a clear positive effect on the quality of the fit. It is important to stress that even the inclusion of the effects of intramolecular potential anharmonicity, would not allow for such a correction. In fact, a calculation based on the Morse potential would only increase the equi-

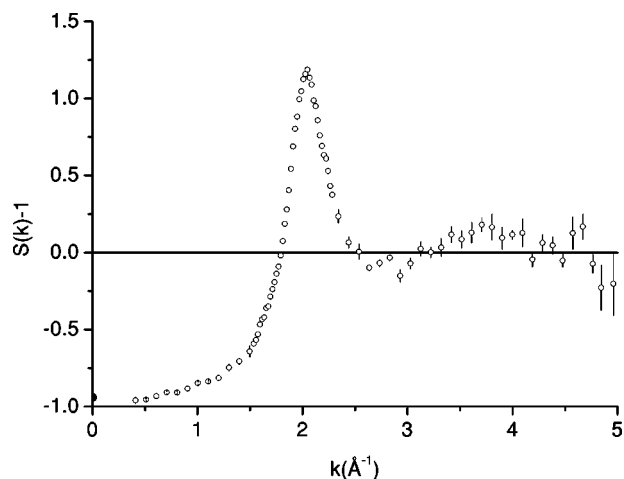


FIG. 2. Measured intermolecular (center-of-mass) structure factor of liquid parahydrogen at $T=17.1$ K and $p=29.9$ bar (open circles with error bars). The value for $S(k=0)$, shown as a black dot, is given in Table I.

librium distance by $\approx 1.2\%$. Thus, the small variation of R_e , used in the present calculation, should be only regarded as a heuristic way of improving the quality of the fit, still using the simple MYK model and a low-power polynomial $P(k^2)$ to account for the residual background (cf. Fig. 1).

Following the procedure just outlined, we were able to determine the center-of-mass structure factor of liquid parahydrogen. This is achieved by subtracting from the data the fitted $B(k)$ and the calculated self-part, obtaining the intermolecular term $(d\sigma/d\Omega)_{\text{dist}}$. As the molecular form factor $u(k)$ is known,³³ the final result for $S(k)$ can be easily derived using Eq. (3). The quantity $S(k)-1$ is shown in Fig. 2 in the range of k between 0 and 5 \AA^{-1} . The data show a peak value of 2.17 for $S(k)$. Then, an undulation is observed with a broad maximum between 3.5 and 4 \AA^{-1} . The shown error bars account for both the statistical uncertainties of the experimental data and the estimated systematic errors introduced by the choice of k_{max} in the fitting procedure. The black dot at $k=0$ represents the compressibility limit, obtained from the thermodynamic data.²¹ The same data treatment was carried out for the other thermodynamic states, obtaining structure factors similar to that of Fig. 2 and shown in Fig. 3.

IV. THE PIMC SIMULATIONS

A set of PIMC simulations was carried out at the same temperatures and densities listed in Table I. The NVT ³⁴ simulations were accomplished using both the isotropic component of the phenomenological pair potential derived by Norman *et al.*³⁵ (NWB) and the semi-empirical isotropic pair potential derived by Silvera and Goldman³⁶ (SG). Both potentials are reliable, with the NWB being more oriented toward the pair interactions and the SG taking into account, in an effective way, the many-body interactions. The PIMC simulations were implemented using the primitive algorithm³⁷ and varying the Trotter number from $P=1$ (clas-

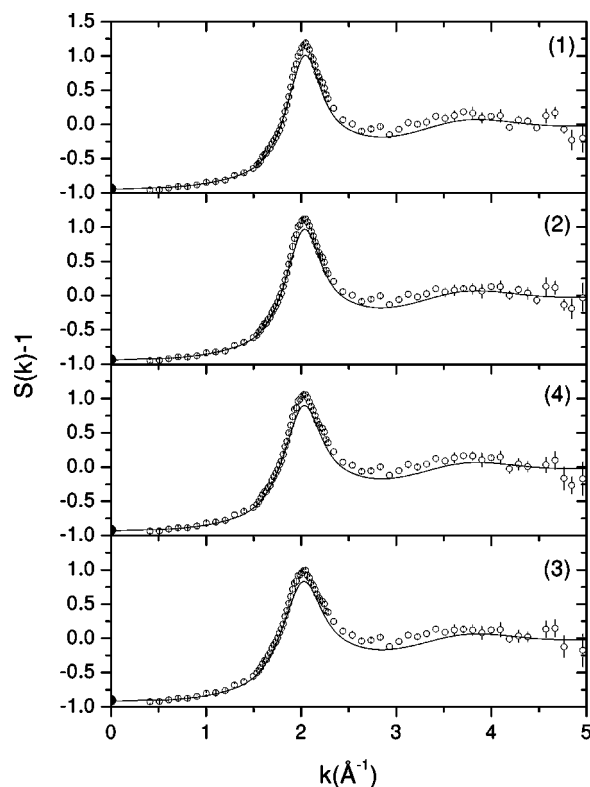


FIG. 3. Comparison between the measured intermolecular (center-of-mass) structure factor of liquid parahydrogen (open circles) and the PIMC simulation results (full lines). The graphs are shown as a function of decreasing density (top to bottom). The black dots at $k=0$ are taken from Table I.

sical limit) to $P=4, 8, 16, 32,$ and 64 in order to check for the convergence of results to the correct quantum-mechanical limit.³⁸ The center-of-mass radial distribution function $g(r)$, simulated with the SG potential, is displayed in Fig. 4 for $P=16$ and $P=32$ in order to show the quality of the convergence to the quantum mechanical limit. The results for P

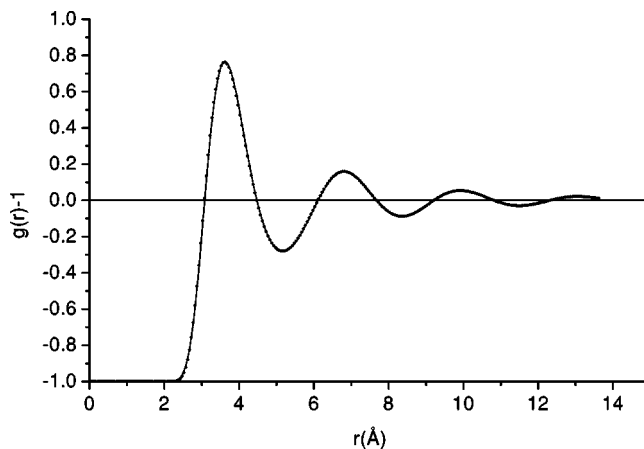


FIG. 4. PIMC results for center of mass $g(r)$ of liquid parahydrogen as a function of the Trotter number. The graph shows the superposition of the results with $P=16$ (dots) and $P=32$ (line) for the thermodynamic point 1, using the SG potential. The $P=32$ and $P=64$ results are indistinguishable, even numerically.

$=32$ and $P=64$ are almost indistinguishable, even at the numerical level.

Only slight differences are obtained if the NWB potential is used. For example, with $P=32$, the peak of $g(r)$ of state 1 is only 1.2 % higher than with the SG model. It should be noted that, while the simulation using the NWB potential gives a negative pressure ($p=-9$ bar), the one with the SG potential produces a positive value ($p=6$ bar) that, however, is still lower than the true experimental value (cf. Table I).³⁹

The center-of-mass radial distribution function produced by the PIMC simulations is limited to intermolecular distances smaller than some maximum value R_{\max} , determined by half the shortest edge-length of the simulation box.⁴⁰ At the investigated densities, we obtain $R_{\max} \approx 13.6$ Å. However, in order to calculate the structure factor, $g(r)$ has to be extrapolated smoothly to r values high enough to avoid truncation effects in the Fourier transform

$$S(k) = 1 + \frac{4\pi n}{k} \int_0^\infty dr r \sin(kr) h(r), \quad (4)$$

where $h(r) = g(r) - 1$.

A simple and well-established procedure of extrapolating $g(r)$ beyond R_{\max} is the recipe by Verlet,⁴¹ who suggests to approximate the asymptotic behavior of $h(r)$ using a damped oscillatory function of the following form:

$$h(r) \sim (A_0/r) \exp(-r/r_0) \sin(r/r_1). \quad (5)$$

The parameters A_0 , r_0 , and r_1 were obtained by fitting the functional form (5) to the simulation results, starting from the third zero of $h(r)$, i.e., at $r \approx 6$ Å. In this way, we could eliminate spurious oscillations in $S(k)$. The structure factors thus obtained are compared with the experimental results in Sec. V.

V. DISCUSSION

The structure-factor data of parahydrogen, obtained from the present experiment according to the procedure described in Sec. III, have been compared to the results of the PIMC simulations outlined in Sec. IV. As we have already discussed, we found no relevant difference in using the two intermolecular potentials, namely, SG and NWB. In the following, we will show the results for the Silvera and Goldman potential. We remind that the simulation conditions were the same of the experiment, i.e., imposing the same temperatures and densities as the ones reported in Table I. As shown in Fig. 3, the agreement is rather good, although the experimental data appear consistently higher than the simulation results in the region of the main peak and up to ≈ 3.5 Å⁻¹. At lower k , the data agree well with the PIMC results.

We have checked the dependence of the main peak height on the fit procedure used to extrapolate $g(r)$. We found no substantial variation of the maximum of $S(k)$ with either changing the fit range for Eq. (5) or using different damped oscillating functions.

A corresponding investigation had previously been carried out on liquid deuterium, in similar thermodynamic conditions and using the NWB intermolecular potential.¹⁰ In that

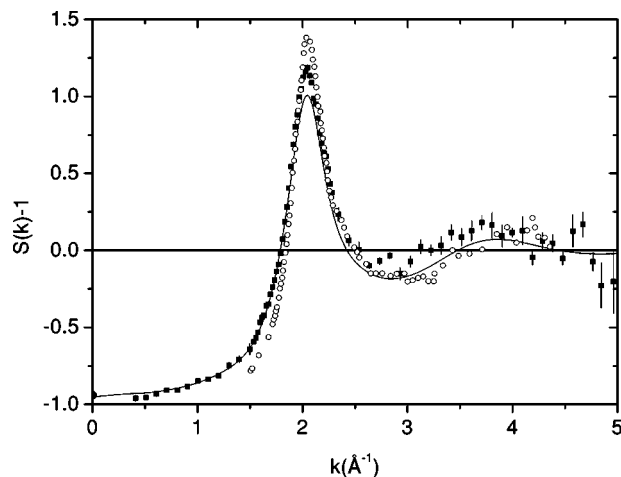


FIG. 5. Comparison between the present experimental determination for state 1 ($T=17.1$ K and $n=22.95$ nm⁻³, full squares with error bars) and the data obtained from Ref. 19 ($T=15.2$ K and $n=22.71$ nm⁻³, open circles). The line represents the present PIMC simulation results. The value at $k=0$ (large black dot) is from Table I.

case, the agreement between simulation and experiment was extremely good. In the present case, an overall quantitative agreement with simulation is also found, although the present experiment appears to be much more difficult and the agreement of a lesser quality.

It is interesting to compare the present structural information to the results of the neutron-diffraction experiment by Dawidowski *et al.*¹⁹ To this aim, we report, in Fig. 5 the present data for state 1 ($T=17.1$ K and $n=22.95$ nm⁻³) with their determination at $T=15.2$ K and $n=22.70$ nm⁻³. We point out that in Ref. 19 only temperature and pressure were given and the density was calculated by us using the equation of state in Ref. 21.

From a careful analysis of Fig. 5, it is interesting to observe that, in spite of the difficulties of both experiments and the different techniques (we remind that the authors of Ref. 19 used a much lower incident neutron energy which implies a totally different data analysis procedure), the two sets of data are consistent on an absolute scale. In the region of the main peak, the experimental determination by Dawidowski *et al.*¹⁹ gives a higher value for the structure factor with respect to the present data which, in turn, are higher than the PIMC results. In the region of the minimum around 3 Å⁻¹, the data of Ref. 19 are closer than ours to the simulation data. By contrast, our experimental data are much closer to the simulation in the low- k region and along the rising edge of $S(k)$. It is difficult to attribute these variations to the slightly different thermodynamic conditions, even though the difference in density is ≈ 1 % and that, in the temperature, is ≈ 12 %. At any rate, by comparing the present simulation results to previous ones,¹⁶ carried out at $T=15.7$ K and $n=22.8$ nm⁻³, we tend to exclude this possibility.

Another interesting comparison can be carried out at the level of the density derivative of $S(k)$ at constant temperature (Fig. 6), using the present data and another independent experimental determination carried out at the neutron-pulsed

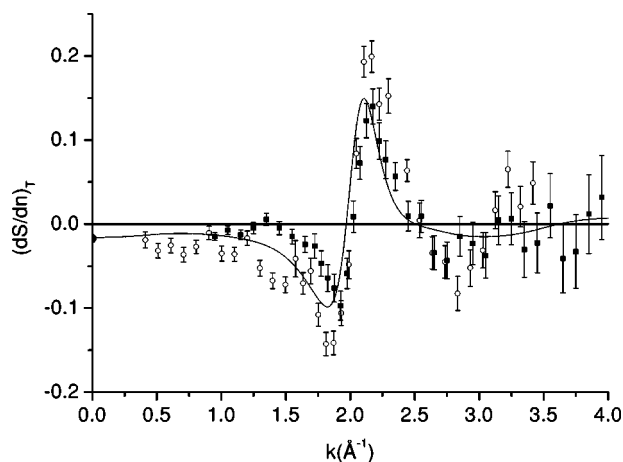


FIG. 6. Density derivative, at constant temperature, of the intermolecular structure factor. Comparison between the present experimental determination (open circles, obtained from the data labeled 1 and 2 in Table I) and the results from Ref. 11 (full squares). The line represents the present PIMC simulation results obtained using the SG potential. The value at $k=0$ (full circle) is obtained from the experimental compressibilities.

source ISIS (U.K.).¹¹ The present results (experiment and PIMC simulation) have been obtained from states 1 and 2 listed in Table I. The two sets of data are consistent with each other, even though some quantitative differences emerge. In the same figure, the line represents the present simulation results.

Looking at Fig. 6, we observe that the previously noted¹¹ variance in the low- k region of the density derivative of $S(k)$ is now counterbalanced by the present experimental results. The PIMC results, which are virtually unchanged passing from SG to NWB potential, appear to average the two experimental sets of data for the density derivative of $S(k)$, in the region below 1.8 \AA^{-1} . In fact, by comparing the simulation results to the weighted average of the two independent experimental results we would obtain a good agreement with PIMC simulation results. Thus, it might be suggested that the two experiments were affected by errors of different origin and that their average is likely to describe the true behavior.

As a final result, we calculated the temperature derivative of $S(k)$ at constant density. As the experiments were not carried out on an isochore, we used the data of states 2 and 4, corresponding to the same pressure. Thus, the temperature derivative was derived using the following expression, both for the experimental and PIMC data:

$$\left(\frac{dS}{dT}\right)_n = \left(\frac{S_4(k) - S_2(k)}{T_4 - T_2}\right) - \left(\frac{dS}{dn}\right)_T \left(\frac{n_4 - n_2}{T_4 - T_2}\right). \quad (6)$$

The result is depicted in Fig. 7, where the present experiment and simulations are represented by open circles and a continuous line, respectively. In the same figure, we also reported the data from another independent measurement (full squares) that had been obtained from the experiment of Ref. 11. The two sets of experimental data results are consistent with each other, although the present ones are affected by larger uncertainties because of the extra contribution from

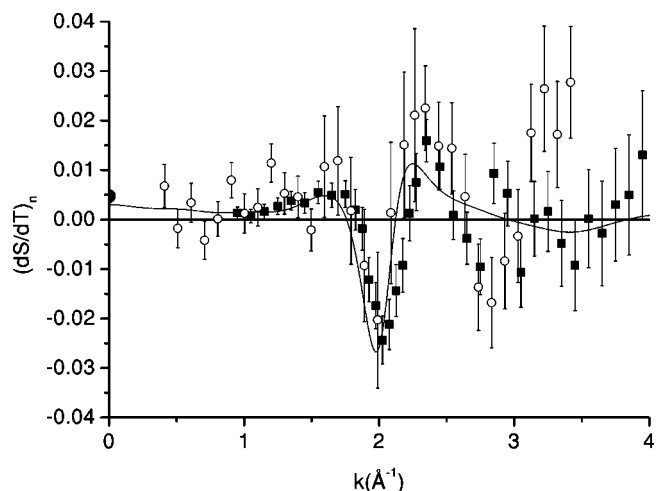


FIG. 7. Temperature derivative, at constant density, of the intermolecular structure factor. Comparison between the present experimental determination (open circles, obtained from the data of states 2 and 4, corrected using the density derivative shown in Fig. 6) and the results from Ref. 11 (full squares). The line represents the present PIMC simulation results, using the SG potential, and obtained using the same procedure as for the experiment data. The value at $k=0$ (full circle) is obtained from the experimental compressibilities.

the errors on the density derivative [cf. Eq. (6)]. We note that the PIMC results quantitatively reproduce the experimental shape. We observe that both the experimental data and the PIMC simulation are consistent with the thermodynamic information derived from the compressibility (large black dot at $k=0$).

VI. CONCLUSIONS

We have reported on the results of a neutron-diffraction experiment by which we have obtained the intermolecular structure factor for liquid parahydrogen. The large self-intramolecular contribution to the scattering has been calculated using an improved model (MYK) for the self part of the dynamic-scattering cross section and subtracted from the data. The same MYK model has been used to compute, by means of a Monte Carlo simulation, the multiple-scattering component. This contribution also has been subtracted from the measured cross section, and we were able to determine the intermolecular (distinct) term that carries the information on the center-of-mass structure factor of liquid parahydrogen. The present results have been compared to the available determinations, in similar thermodynamic conditions, published in the literature and with our own PIMC simulation results. The comparison, as far as the experimental data are concerned, is satisfactory, especially considering the difficulty of the experiments. Neither set of data appears to be in full agreement with the PIMC results, with the present determination closer to the simulation results in the low-momentum region up to the first peak, and the data of Ref. 19 more consistent with the PIMC results in the region of the minimum around 3 \AA^{-1} .

The density derivative of the structure factor obtained from the present data has been also compared to previous results obtained from a pulsed neutron-diffraction experiment. Also in this case, the comparison between the experimental results is quantitatively satisfactory. The previously observed¹¹ variance between the experiment and simulation, noted in the low- k region of the density derivative of $S(k)$, comes out reversed in the present results and is likely to be attributed to residual systematic errors, which we were unable to eliminate in both experiments. This suggests that the PIMC simulation is probably giving a correct description of this part of the distribution. The present results on the temperature derivative of $S(k)$ confirm the previous determination and agree with the PIMC simulation.

The overall convergence between the various experimental determinations of $S(k)$, obtained by the different groups,

is a positive indication of the increasing accuracy of the experimental techniques, but calls for a further improvement of the neutron-diffraction techniques to definitely solve the problem of an accurate determination of the static structure factor of molecular hydrogen in the liquid state. This remains a long-standing objective in physics of liquid matter, whose fundamental and applicative involvements are self-evident nowadays.

ACKNOWLEDGMENTS

The skillful technical assistance of Pierre Palleau (ILL, Grenoble, France) is gratefully acknowledged. This work has been partially supported by the Istituto di Fisica della Materia (Italy) and by the Ente Cassa di Risparmio di Firenze (Project Firenze-Hydrolab).

-
- ¹F. Barocchi, M. Neumann, and M. Zoppi, *Phys. Rev. A* **31**, 4015 (1985).
²F. Barocchi, M. Neumann, and M. Zoppi, *Phys. Rev. A* **36**, 2440 (1987).
³E. Rabani and D. R. Reichman, *J. Chem. Phys.* **116**, 6271 (2002).
⁴T. D. Hone and G. A. Voth, *J. Chem. Phys.* **121**, 6412 (2004).
⁵U. Balucani and M. Zoppi, *Dynamic of the Liquid State* (Clarendon Press, Oxford, 1994).
⁶G. Placzek, *Phys. Rev.* **86**, 377 (1952).
⁷M. Zoppi, U. Bafile, R. Magli, and A. K. Soper, *Phys. Rev. E* **48**, 1000 (1993).
⁸M. Zoppi, A. K. Soper, R. Magli, F. Barocchi, U. Bafile, and N. W. Ashcroft, *Phys. Rev. E* **54**, 2773 (1996).
⁹E. Guarini, F. Barocchi, R. Magli, U. Bafile, and M. C. Bellissent-Funel, *J. Phys.: Condens. Matter* **7**, 5777 (1995).
¹⁰M. Zoppi, U. Bafile, E. Guarini, F. Barocchi, R. Magli, and M. Neumann, *Phys. Rev. Lett.* **75**, 1779 (1995).
¹¹M. Zoppi, M. Celli, and A. K. Soper, *Phys. Rev. B* **58**, 11 905 (1998).
¹²J. de Boer, *Rep. Prog. Phys.* **12**, 305 (1949).
¹³I. F. Silvera, *Rev. Mod. Phys.* **52**, 393 (1980).
¹⁴F. J. Bermejo, K. Kinugawa, C. Cabrillo, S. M. Bennington, B. Fåk, M. T. Fernández-Díaz, P. Verkerk, J. Dawidowski, and R. Fernández-Perea, *Phys. Rev. Lett.* **84**, 5359 (2000).
¹⁵S. W. Lovesey, *Theory of Neutron Scattering from Condensed Matter*, Vol. 1 (Oxford University Press, Oxford, 1987).
¹⁶M. Zoppi, M. Neumann, and M. Celli, *Phys. Rev. B* **65**, 092204 (2002).
¹⁷For a review on the quantum simulation techniques see e.g.: D. M. Ceperley, *Rev. Mod. Phys.* **67**, 279 (1995).
¹⁸J. P. Hansen and L. Verlet, *Phys. Rev.* **184**, 151 (1969).
¹⁹J. Dawidowski, F. J. Bermejo, M. L. Ristig, B. Fåk, C. Cabrillo, R. Fernández-Perea, K. Kinugawa, and J. Campo, *Phys. Rev. B* **69**, 014207 (2004).
²⁰A. Cunsolo, G. Pratesi, D. Colognesi, R. Verbeni, M. Sampoli, F. Sette, G. Ruocco, R. Senesi, M. H. Krisch, and M. Nardone, *J. Low Temp. Phys.* **129**, 117 (2002).
²¹H. M. Roder, G. E. Childs, R. D. McCarty, and P. E. Angerhofer, NBS Tech. Note n. 641 (1973).
²²F. Barocchi, P. Chieux, R. Fontana, R. Magli, A. Meroni, A. Parola, L. Reatto, and M. Tau, *J. Phys.: Condens. Matter* **9**, 8849 (1997).
²³M. Celli, M. Zoppi, N. Rhodes, and A. K. Soper, *J. Phys.: Condens. Matter* **11**, 10229 (1999).
²⁴J. P. Hansen and I. R. McDonald, *Theory of Simple Liquids*, 2nd ed. (Academic, London, 1986), Chap. 12.
²⁵J. A. Young and J. U. Koppel, *Phys. Rev.* **A135**, 603 (1964).
²⁶J. Van Kranendonk, *Solid Hydrogen* (Plenum, New York, 1983).
²⁷M. Zoppi, L. Ulivi, M. Santoro, M. Moraldi, and F. Barocchi, *Phys. Rev. A* **53**, R1935 (1996).
²⁸M. Moraldi, M. Santoro, L. Ulivi, and M. Zoppi, *Phys. Rev. B* **58**, 234 (1998).
²⁹W. Langel, D. L. Price, R. O. Simmons, and P. E. Sokol, *Phys. Rev. B* **38**, 11 275 (1988).
³⁰M. Celli, D. Colognesi, and M. Zoppi, *Eur. Phys. J. B* **14**, 239 (2000).
³¹K. P. Huber and G. Herzberg, *Constants of Diatomic Molecules* (Van Nostrand, New York, 1979).
³²H. H. Paalman and C. J. Pings, *J. Appl. Phys.* **33**, 2635 (1962).
³³M. Zoppi, *Physica B* **183**, 235 (1993).
³⁴In the present simulations we always used a fixed number ($N=560$) of classical particles. The volume of the simulation box (V) was determined by N and the densities listed in Table I.
³⁵M. J. Norman, R. O. Watts, and U. Buck, *J. Chem. Phys.* **81**, 3500 (1984).
³⁶I. F. Silvera and V. V. Goldman, *J. Chem. Phys.* **69**, 4209 (1978).
³⁷M. P. Allen and D. J. Tildesley, *Computer Simulation of Liquids* (Clarendon Press, Oxford, 1987).
³⁸M. Neumann and M. Zoppi, *Phys. Rev. A* **44**, 2474 (1991).
³⁹These values are relative to $P=32$. The extrapolation carried out using the $P=64$ value produces, for the SG case and for state 1, a limit value for the pressure $p \approx 12$ bar.
⁴⁰As the simulations were started from an *hcp* crystal of parahydrogen, the box is almost, but not exactly, cubic.
⁴¹L. Verlet, *Phys. Rev.* **165**, 201 (1968).